Article

UDC 544.42+519.242.7

https://doi.org/10.31489/2025PH3/95-106

Received: 21.03.2025
Accepted: 24.06.2025

S.N. Hosseinimotlagh[1], M.A. Zarei[2], A. Shakeri[1]✉

[1]*Department of Physics, Shi.C., Islamic Azad University, Shiraz, Iran;*
[2]*Department of Physics, Payame Noor University, Tehran, Iran*

Control Method of Plasma Burning in Tokamak Fusion Reactor with Neutron-Free $p^{11}B$ Fuel via Alpha-Proton-Alpha Avalanche Reaction Mechanism

This article deals with the problems of neutronic fuels. The characteristic features of plasma burning control in tokamak fusion reactor with neutron-free $p^{11}B$ fuel via alpha-proton-alpha avalanche reaction are analyzed. On the basis of the study the author suggests, a model with no dimensions for plasma ignition, where equations for particle and energy equilibrium are utilized. In this framework $p^{11}B$ fuel are considered. In fact, this work presents a novel method to control the burning plasma such that we can control the system variations, the rate of fueling and supplementary power. Applying the simulation equations and we calculate quality factor for $p^{11}B$ fuel. The neutronic fuels come with two main drawbacks: (i) they generate neutrons that necessitate protection and can harm and activate the reactor's structure, (ii) the production of tritium involves added complexity, expense, and the need for radial space for a lithium blanket. It has been demonstrated that the neutron-free $p^{11}B$ reaction is often regarded as a potential remedy for these issues.

Keywords: plasma, fusion, dynamics, neutron-free, energy, control, avalanche, alpha, proton, fuel

✉*Corresponding author*: Abuzar Shakeri, Abuzar.Shakeri@gmail.com

Introduction

Managing plasma density and temperature within fusion reactors constitutes one of the key challenges in advancing this technology. The source of instability arises from the fact that, with lower temperatures, fusion heating enhances as plasma temperature rises. To maintain stability at such operational levels in fusion reactors, a dynamic control system will be crucial. Throughout the years, various techniques for managing the burn conditions have been explored. Among these studies, three specific forms of actuation have been identified: (i) deliberate impurities injection, (ii) fueling rate adjustment, and (iii) power of supplementary [1–3]. Control systems that rely on altering the supplementary power function necessitate functioning at sub-ignition levels where the supplementary power is active [4–6]. When the plasma temperature increases due to a positive initial temperature fluctuation, the control system decreases the supplementary power output. Conversely, managing negative initial temperature fluctuations is less complex, primarily depending on having sufficient heating capacity. Control systems that adjust the fueling rates enable functioning at ignition levels where supplementary power remains inactive [7–11].

Despite their capability to manage disruptions in starting conditions that result in thermal excursions, they struggle with disturbances in starting conditions that cause quenching. Intentionally introducing impurities can effectively amplify radiation losses within the plasma, serving to avert thermal excursions. When faced with significant positive shifts in the initial temperature, this strategy necessitates a substantial quantity of impurities. Consequently, once the thermal excursion is regulated, extra supplementary power must be supplied, which leads to a decrease in Q, to counteract the radiation losses brought about by the impurities until they are entirely eliminated from the reactor. Previous studies have studied the control of plasma burning in a tokamak fusion reactor with D^3He and DT fuel. However, the innovative design of this work is that we study the method of controlling the burning of neutron-free $p^{11}B$ plasma through the alpha-proton-alpha avalanche reaction mechanism.

The main objective of the article is checking the burning plasma stability conditions in fusion reactor for $p^{11}B$ fuel. Therefore, the paper is organized as follows. In Section.2 fuel selection consideration is introduced. Section.3, indicates a zero-dimensional burning plasma model. Section.4, indicates the control meth-

ods. In section.5, we discus on the simulation parameters and results, for selected fuels ($p^{11}B$). Section.6, summarizes the conclusions.

Two different fuel combinations, DT and $p^{11}B$, are viewed as the most promising options for achieving functional fusion reactors in the near future.

$$D + T \rightarrow n + {}^{4}He$$

$$p + {}^{11}B \rightarrow 3\,{}^{4}He$$

Although DT is the most common fuel used for fusion reactor but $p^{11}B$ fuel is considered in this work due to the advantages of reduced radioactivity, reduced radiation damage, increased safety and efficiency, lower cost of electricity and potentially shorter path to commercialization $p^{11}B$ fuel.

Managed fusion with sophisticated fuels, especially hydrogen-boron-11, stands out as an incredibly promising energy source. This hydrogen-boron fuel mainly generates energy as charged particles rather than neutrons, which greatly lowers or could even eradicate induced radioactivity. The principal reaction, $p + {}^{11}B \rightarrow 3\,{}^{4}He$, results solely in charged particles. In addition, a secondary reaction, ${}^{4}He + {}^{11}B \rightarrow {}^{14}N + n$, generates neutrons as the alpha particles created by the principal reaction decelerate within the plasma; however, these neutrons account for just about 0.2 % of the overall fusion energy, with an average energy of only 2.5 MeV.

Zero-dimensional burning plasma model using alpha-proton-alpha avalanche reaction mechanism

As illustrated in Figure 1, the processes involved in the $p^{11}B$ avalanche reaction that generates a surge of alpha particles include: [19] (i): an alpha particle produced from the fusion of $p^{11}B$ strikes a proton that is stationary in the laboratory setting. (ii): This alpha particle subsequently collides with a second proton in the surrounding medium, which is also at rest. The resulting energetic proton then engages with one ^{11}B atom in the environment, which remains stationary. (iii): This leads to the formation of three additional alpha particles. So that:

$$(\mathrm{i}): \mathrm{p} + \mathrm{B}^{11} \rightarrow \alpha_1 + \alpha_2 + \alpha_3;;$$

$$(\mathrm{ii}): \alpha_1 + \mathrm{H}(\mathrm{rest.lab}) \rightarrow \alpha_1' + p' + e$$

$$(\mathrm{iii}): \mathrm{p}' + {}^{11}\mathrm{B}(\mathrm{rest.lab}) \rightarrow \alpha_1 + \alpha_2 + \alpha_3 + 11e\,.$$

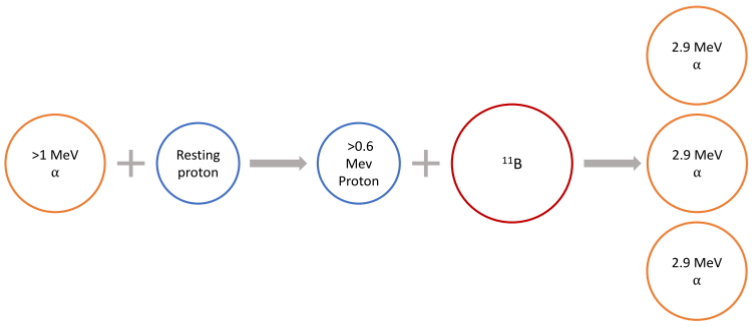

Figure 1. Exploring the mechanism of the α-p-α avalanche reaction. When an α particle strikes a resting proton, this proton gains sufficient energy to engage with ^{11}B, resulting in the generation of three α particles

These three α particles can once more generate accelerated protons, leading to an avalanche of α particles. The equations that describe the coupled nonlinear point kinetics of the $p^{11}B$ fusion reaction, taking into account the alpha-proton-alpha avalanche process, can be expressed as follows:

In this work, a model with zero dimensions is utilized for the process of plasma ignition, employing the equations for particle and energy equilibrium [12, 13]. Within this framework, the characteristics of $p^{11}B$ fuel and its density are evaluated independently, enabling us to identify appropriate isotopic fuels suitable for use as an actuator. The representation of the model can be illustrated through these equations:

$$\frac{dn_\alpha}{dt} = -\frac{n_\alpha}{\tau_\alpha} + 3n_p n_{^{11}B} \langle \sigma v \rangle \qquad (1)$$

$$\frac{dn_{\mathrm{p}}}{dt} = -\frac{n_{\mathrm{p}}}{\tau_{\mathrm{p}}} - n_{\mathrm{p}} n_{^{11}\mathrm{B}} \langle \sigma v \rangle + n_{\mathrm{p}} n_{\alpha} \sigma_{el} v_{\alpha} + S_{\mathrm{p}}, \tag{2}$$

$$\frac{dn_{^{11}\mathrm{B}}}{dt} = -\frac{n_{^{11}\mathrm{B}}}{\tau_{^{11}\mathrm{B}}} - n_{\mathrm{p}} n_{^{11}\mathrm{B}} \langle \sigma v \rangle + S_{^{11}\mathrm{B}}, \tag{3}$$

$$\frac{dE}{dt} = -\frac{E}{\tau_E} + Q_{\alpha} n_{\mathrm{p}} n_{^{11}\mathrm{B}} \langle \sigma v \rangle - P_{rad} + P_{aux} + P_{ohmic}, \tag{4}$$

here σ_{el} denotes the elastic cross-section and v_{α} is the proton-alpha relative velocity before the elastic collision. In the above equations, $n_{\alpha}, n_p, n_{^{11}\mathrm{B}}$ are the alpha, hydrogen, and boron 11 particle densities respectively, and E signifies energy. $\tau_{^{11}\mathrm{B}}, \tau_p, \tau_{\alpha}, \tau_E$ are boron 11, hydrogen, alpha, particles along with energy confinement duration, respectively, that are connected by relationships: $\tau_{\alpha} = k_{\alpha}\tau_E, \tau_p = k_p\tau_E, \tau_{^{11}\mathrm{B}} = k_{^{11}\mathrm{B}}\tau_E$ parameters of which k_{α}, k_p and $k_{^{11}\mathrm{B}}$ are listed in the Table 1. The energy confinement duration scaling referenced in this research focuses on ITER90H-P [14]. The design of the controller does not rely on this scaling, and the scaling applied is:

$$\tau_{\mathrm{E}} = f\, 0.082 I^{1.02} R^{1.6} B^{0.15} A_i^{0.5} \kappa_x^{-0.19} P^{-0.47}, \tag{5}$$

f is scaling factor and established by evaluating the relationship between the power required for the L-H transition and the overall plasma heating power P. In this work, the system operates continuously in H-mode, and we set f to 0.85 for our simulation purposes. The quantities R, I, κ_x, and B remain fixed and are given in Table 1.

The isotopic number $A_i = 3\gamma + 2(1-\gamma) = \gamma + 2$ ($\gamma = \dfrac{n_{^{11}\mathrm{B}}}{n_p + n_{^{11}\mathrm{B}}}$ is boron 11 densities fraction which is equal to 2.5 for the 50:50 $\mathrm{p}^{11}\mathrm{B}$ mixture). P_{rad} is radiation loss which approximated as:

$$P_{rad} = P_{brem} = A_b Z_{eff} n_e^2 \sqrt{T}. \tag{6}$$

Where $A_{b\left(p^{11}B\right)} = 5.35\times10^{-37}\dfrac{Wm^3}{\sqrt{KeV}}$, $Z_{eff} = \sum_i \dfrac{n_i Z_i^2}{n_e} = \dfrac{n_p + n_{^{11}\mathrm{B}} + 4n_{\alpha}}{n_e}$ and $n_e = n_p + n_{^{11}\mathrm{B}} + 2n_{\alpha}$ refers to the coefficients associated with bremsstrahlung radiation [15], the effective atomic number, and the density of electrons respectively. Also, Z_i denotes the atomic number of different ions. $\langle \sigma v \rangle$ is known as fusion reactivity which is temperature dependent and calculated by:

$$\langle \sigma v \rangle = C_1 \zeta^{-5/6} \xi^2 \exp\left(-3\zeta^{1/3}\xi\right) + 5.41\times10^{-15} T^{-3/2} \times \exp\left(-\frac{148}{T}\right),$$

$$\zeta = 1 - \frac{C_2 T + C_4 T^2 + C_6 T^3}{1 + C_3 T + C_5 T^2 + C_7 T^3},$$

$$\xi = C_0 / T^{1/3}. \tag{7}$$

Where the parameter C_i is found in [16]. $S_{^{11}\mathrm{B}}$ and S_p are boron 11 and the hydrogen fueling injection rates as control inputs, and P_{aux} is supplementary heating in the fuel of $\mathrm{p}^{11}\mathrm{B}$.

Q_{α} denotes α-particles energy, where $Q_{\alpha}\left(\mathrm{p}^{11}B\right) = 2.9\,\mathrm{MeV}$ for $\mathrm{p}^{11}\mathrm{B}$ fusion reaction [17]. P_{ohmic} (Ohmic power) is given by:

$$P_{ohmic} = \eta j^2 \tag{8}$$

Here:

$$\eta = \ln\left(\frac{T^{3/2}}{\sqrt{\pi} Z_{eff} e^3 \sqrt{n}}\right) \times 1.03\times10^{-4} \times T^{-3/2} Z_{eff}, \tag{9}$$

η is referred to as Spitzer resistivity while *j* denotes the current density of plasma. In the equation (9), *T* is measured in Kelvin [18]. The temperature, the total power of plasma heating *P*, and the density plasma are expressed as follows:

$$T = \frac{2}{3}\frac{E}{n} \tag{10}$$

$$P = P_{fusion} - P_{rad} + P_{aux} + P_{ohmic} \tag{11}$$

$$n = 2n_p + 2n_{^{11}\mathrm{B}} + 3n_\alpha \tag{12}$$

Where fusion power for $p^{11}B$ fuel is given by:

$$P_{fusion} = Q_\alpha n_p n_{^{11}\mathrm{B}} \langle \sigma v \rangle = Q_\alpha \gamma (1-\gamma) n^2_{\mathrm{p}^{11}B} \langle \sigma v \rangle \tag{13}$$

Such that: $n_{p^{11}B} = n_p + n_{^{11}\mathrm{B}}$ is the summation of first and second fuel densities.

Table 1

Parameters of reactor

1)	Plasma volume (m^3)	$V = 1500$
2)	Plasma current (MA)	$I = 24$
3)	Minor radius (m)	$a = 3.8$
4)	Major radius (m)	$R = 14$
5)	Boron 11 (Helium 3) particle confinement constant	$k_{^{11}\mathrm{B}} = 2.6$
6)	Hydrogen particle confinement	$k_{\mathrm{p}} = 3.6$
7)	Alpha particle confinement constant	$k_\alpha = 7$
8)	Magnetic field (T)	$B = 3.5$
9)	Elongation at χ (κ_x)	$\kappa_x = 2.2$

The equilibrium numerical values for various densities, $\bar{n}_{^{11}\mathrm{B}}$, $\bar{n}_\alpha$, $\bar{n}_p$, energy, $\bar{E}$, along with the source of fueling terms $\bar{S}_{^{11}\mathrm{B}}$, $\bar{S}_p$ and the auxiliary (supplementary) heating $\bar{P}_{aux}$, are established by solving a set of nonlinear equations obtained by setting the left side of equations 1–4 to zero. It is important to mention that in these equations, the variables $\bar{\beta} = \frac{knT}{B^2/2\mu_0}$, $\bar{\gamma}$, and $\bar{T}$ are selected randomly [19].

$$0 = -\frac{\bar{n}_\alpha}{\bar{\tau}_\alpha} + \bar{n}_p \bar{n}_{^{11}\mathrm{B}} \langle \overline{\sigma v} \rangle \tag{14}$$

$$0 = -\frac{\bar{n}_p}{\bar{\tau}_p} - \bar{n}_p \bar{n}_{^{11}\mathrm{B}} \langle \overline{\sigma v} \rangle + \bar{S}_p \tag{15}$$

$$0 = -\frac{\bar{n}_{^{11}\mathrm{B}}}{\bar{\tau}_{^{11}\mathrm{B}}} - \bar{n}_p \bar{n}_{^{11}\mathrm{B}} \langle \overline{\sigma v} \rangle + \bar{S}_{^{11}\mathrm{B}} \tag{16}$$

$$0 = -\frac{\bar{E}}{\bar{\tau}_E} + Q_\alpha \bar{n}_p \bar{n}_{^{11}\mathrm{B}} \langle \overline{\sigma v} \rangle - \bar{P}_{rad} + \bar{P}_{aux} + P_{ohmic} \tag{17}$$

For arbitrarily values of $\bar{\beta}, \bar{\gamma}, \bar{T}$, equilibrium values $\bar{n}_\alpha, \bar{n}_p, \bar{n}_{^{11}\mathrm{B}}, \bar{E}, \bar{S}_p, \bar{S}_{^{11}\mathrm{B}}, \bar{P}_{aux}$ calculated from equations 14–17 are shown in Table 2 [20]. Defining the difference from the average values as: $n_{^{11}\mathrm{B}} - \bar{n}_{^{11}\mathrm{B}}$, $\tilde{n}_\alpha = n_\alpha - \bar{n}_\alpha$, $\tilde{n}_p = n_p - \bar{n}_p$, $\tilde{E} = E - \bar{E}$, therefore, the equations describing the changes can be formulated as:

$$\frac{d\tilde{n}_\alpha}{dt} = -\frac{\tilde{n}_\alpha}{\tau_\alpha} - \frac{\overline{n}_\alpha}{\tau_\alpha} + S_\alpha \tag{18}$$

$$\frac{d\tilde{n}_p}{dt} = -\frac{\tilde{n}_p}{\tau_p} - \frac{\overline{n}_p}{\tau_p} - S_\alpha + S_D \tag{19}$$

$$\frac{d\tilde{n}_{^{11}\mathrm{B}}}{dt} = -\frac{\tilde{n}_{^{11}\mathrm{B}}}{\tau_{^{11}\mathrm{B}}} - \frac{\overline{n}_{^{11}\mathrm{B}}}{\tau_{^{11}\mathrm{B}}} - S_\alpha + S_{^{11}\mathrm{B}} \tag{20}$$

$$\frac{d\tilde{E}}{dt} = -\frac{\tilde{E}}{\tau_E} - \frac{\overline{E}}{\tau_E} + Q_\alpha S_\alpha - P_{rad} + P_{aux} + P_{ohmic} \tag{21}$$

To simplify S_α is written as follows:

$$S_\alpha\left(E, n_\alpha, n_p, n_{^{11}\mathrm{B}}\right) = n_p n_{^{11}\mathrm{B}} \sigma v = \gamma\left(1-\gamma\right) n_{p^{11}\mathrm{B}}^2 \sigma v \tag{22}$$

Notice that, $\langle \sigma v \rangle$ is a function of $n_{^{11}\mathrm{B}}, n_p, n_\alpha, E$. The starting fluctuations $\tilde{n}_{^{11}\mathrm{B}}, \tilde{n}_p$, $\tilde{n}_\alpha$, $\tilde{E}$ are compelled to become zero, and this research is accomplished through the adjustment of the fuel sources ($S_{^{11}\mathrm{B}}$ and S_p) and the supplemental energy (P_{aux}).

Table 2

Equilibrium point

$\overline{T}$	Temperature	250 keV
$\overline{\beta}$	Plasma Beta	93 %
$\overline{n}_p$	Density of Hydrogen Density	1.2×10^{19} m^{-3}
$\overline{n}$	Total Density	9.44×10^{19} m^{-3}
$\overline{n}_\alpha$	Density of Alpha particle Density	$1.53\times10^{19}\,\mathrm{m}^{-3}$
$\overline{S}_\mathrm{p}$	Hydrogen Fueling Rate	1.30×10^{17} $\mathrm{m}^{-3}\mathrm{s}^{-1}$
$\overline{S}_{^{11}\mathrm{B}}$	Boron 11 Fueling Rate	1.60×10^{17} $\mathrm{m}^{-3}\mathrm{s}^{-1}$
$\overline{P}_{aux}$	Supplementary Power	1.80×10^{5} $\mathrm{W/m}^3$
$\overline{P}$	Net plasma power	$1.59\times10^{5}\,\mathrm{W/m}^3$
$\overline{E}$	Energy Density	$6.7\times10^{6}\,\mathrm{J/m}^{-3}$
$\overline{\gamma}$	Boron 11 Fraction	0.5

Control methods

The controllers operate at sub-ignition and ignition points. Controllers that rely on the modulation of supplementary power must function at sub-ignition levels, where the supplementary power is not zero. In contrast, when the controllers adjusted by the fueling rate are utilized, they can operate at ignition points where the supplementary power is zero. In the following both cases can be considered. First, to stabilize the energy the following conditions put in equation (21):

$$Q_\alpha S_\alpha - P_{rad} + P_{aux} + P_{ohmic} = \frac{\overline{E}}{\tau_E} \tag{23}$$

The equation (21) is satisfied and written as follows:

$$\frac{d\tilde{E}}{dt} = -\frac{\tilde{E}}{\tau_E} \tag{24}$$

$\tilde{E}$ demonstrates exponential stability as τ_E is greater than zero. Condition (23) is satisfied by adjusting the α -heating component $Q_\alpha S_\alpha$ and the supplementary heating. We can manipulate the α -heating term by

changing the ratio $\gamma = \frac{n_{^{11}\mathrm{B}}}{n_p + n_{^{11}\mathrm{B}}}$ in the plasma. Stabilization control is performed in according to the following steps:

1) Beginning in equation (23), we set $P_{aux} = 0$, $\gamma = \gamma^*$ and to solve this equation for γ^*:

$$Q_\alpha \gamma^* \left(1 - \gamma^*\right) - P_{rad} + P_{ohmic} = \frac{\bar{E}}{\tau_E} \tag{25}$$

$$\gamma^* \left(1 - \gamma^*\right) = \frac{\frac{\bar{E}}{\tau_E} + P_{rad} - P_{ohmic}}{Q_\alpha n_{p^{11}B}^2 \langle \sigma v \rangle} = C \tag{26}$$

$$\gamma^* = \frac{1 \mp \sqrt{1 - 4C}}{2} \tag{27}$$

If $C \le 0.25$, the two resulting solutions for γ^* are real and less than 0.5 and would be acceptable. If $C > 0.25$, there is no real answer and we are moving on to the second step.

2) If $\gamma^* = 0.5$, simply adjusting the γ ratio will not satisfy condition (23), thus requiring changes through heating. To achieve this, the supplementary power is determined as follows:

$$P_{aux} = \frac{\bar{E}}{\tau_E} - n_{p^{11}B}^2 \sigma v Q_\alpha \gamma^* \left(1 - \gamma^*\right) - P_{ohmic} + P_{rad} \tag{28}$$

In accordance with the control aims and prior stages, ideal benchmark values for the energy $\bar{E}$ and the fraction of fuel particles γ^* are established.

According to obtained dynamical equations in above, we choose Lyapunov function as follows:

$$V = \frac{k_1^2 \tilde{E}^2 + k_2^2 \hat{\gamma}^2 + \tilde{n}_{p^{11}B}^2}{2} \tag{29}$$

Where $k_1 = 10^{15}$, $k_2 = 10^{20}$ and the derivative of Lyapunov function $\dot{V}$ with simplification is as follows:

$$\dot{V} = -\frac{k_1^2 \tilde{E}^2}{\tau_E} + \frac{k_2^2 \hat{\gamma}}{n_{p^{11}\mathrm{B}}} \left[\frac{k_1^2 n_{p^{11}B} \tilde{E} \phi}{k_2^2} - \frac{n_{^{11}\mathrm{B}}}{\tau_{^{11}\mathrm{B}}} - S_\alpha + S_{^{11}\mathrm{B}} - n_{p^{11}\mathrm{B}} \dot{\gamma}^* - \gamma \left(-\frac{n_{^{11}\mathrm{B}}}{\tau_{^{11}\mathrm{B}}} - \frac{n_p}{\tau_p} - 2S_\alpha + S_D + S_{^{11}\mathrm{B}} \right) \right] + \\ + \tilde{n}_{p^{11}\mathrm{B}} \left[-\frac{n_{^{11}\mathrm{B}}}{\tau_{^{11}\mathrm{B}}} - \frac{n_p}{\tau_p} - 2S_\alpha + S_p + S_{^{11}\mathrm{B}} \right] \tag{30}$$

By stabilizing of equation (30):

$$S_p = \frac{n_{^{11}\mathrm{B}}}{\tau_{^{11}\mathrm{B}}} + \frac{n_p}{\tau_p} + 2S_\alpha - S_{^{11}\mathrm{B}} - K_p \tilde{n}_{p^{11}\mathrm{B}} \tag{31}$$

Where $K_D > 0$. This selection reduces equation (30) to:

$$\dot{V} = \frac{k_2^2 \hat{\gamma}}{n_{p^{11}\mathrm{B}}} \left[\frac{k_1^2 n_{p^{11}\mathrm{B}} \tilde{E} \phi}{k_2^2} - \frac{n_{^{11}\mathrm{B}}}{\tau_{^{11}\mathrm{B}}} - S_\alpha + S_{^{11}\mathrm{B}} - n_{p^{11}\mathrm{B}} \dot{\gamma}^* + K_p \tilde{n}_{p^{11}\mathrm{B}} \gamma \right] - \frac{k_1^2 \tilde{E}^2}{\tau_E} - K_p \tilde{n}_{p^{11}\mathrm{B}}^2 \tag{32}$$

Finally, we take:

$$S_{^{11}\mathrm{B}} = -\frac{k_1^2 n_{p^{11}\mathrm{B}} \tilde{E} \phi}{k_2^2} + \frac{n_{^{11}\mathrm{B}}}{\tau_{^{11}\mathrm{B}}} + S_\alpha + n_{p^{11}\mathrm{B}} \dot{\gamma}^* - K_p \tilde{n}_{p^{11}\mathrm{B}} \gamma - K_{^{11}\mathrm{B}} \hat{\gamma} \tag{33}$$

$$S_p = \frac{k_1^2 n_{p^{11}\mathrm{B}} \tilde{E} \phi}{k_2^2} + \frac{n_p}{\tau_p} + S_\alpha - n_{p^{11}\mathrm{B}} \dot{\gamma}^* - K_p \tilde{n}_{p^{11}\mathrm{B}} \left(1 - \gamma\right) + K_{^{11}\mathrm{B}} \hat{\gamma} \tag{34}$$

The results of the calculations are shown in the next section.

Results and Discussion

In the study of nuclear fusion, the Lawson criterion, initially formulated for fusion reactors, serves as a crucial standard for assessing the circumstances required for a fusion reactor to ignite. Achieving this condition means that the energy produced from the fusion reactions can effectively heat the plasma enough to keep its temperature stable despite any losses, all without the need for external energy sources. This criterion can be expressed as follows:

$$n\tau_E \geq \frac{12T(\text{keV})}{Q_\alpha \langle \sigma v \rangle} \tag{35}$$

The results of Lawson criterion calculation for $p^{11}B$ fuel are shown in Figure 2. As seen in Figure 2, Lawson criterion is true for $p^{11}B$ fuel.

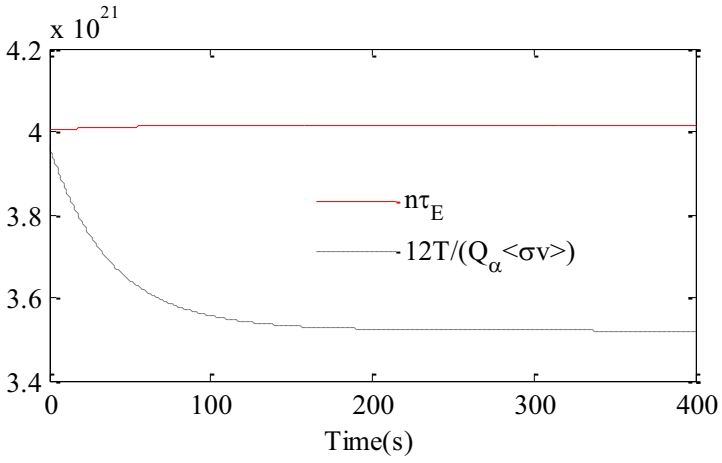

Figure 2. Lawson criterion for $p^{11}B$ fuel

The simulation in this work is performed for the initial values $E(0)=1.2\bar{E}$, $n_\alpha(0)=1.2\bar{n}_\alpha$, $\gamma(0)=.88\bar{\gamma}$, $n_{p^{11}B}(0)=.8\bar{n}_{p^{11}B}$. It has been observed that a controller is capable of adjusting its inputs to achieve the intended result on the system's output. A specific kind of control system, where the output does not affect the input signal's control actions, is known as an open loop system (Fig. 3). This type of system is characterized by the absence of measurement or feedback of the output signal or condition for evaluating against the input signal. Thus, these systems are often labeled as non-feedback systems. Moreover, since an open loop system lacks feedback to verify if the intended output was reached, it operates on the assumption that the input's target was met, as it is unable to rectify any potential errors and cannot adjust for any external influences on the system.

Figure 3. Open loop state

In the simulation of open loop, the system is first fluctuated, while the actuators ($S_{^{11}B}$, P_{aux}, S_p) maintain their steady-state values (Table 2) as equations (1–4) are resolved. The results of the simulation indicate that in the absence of active control, a thermal deviation arises, causing the system to stray from the intended equilibrium point. Figure 5 (dotted-black) illustrates the changes in the states over time.

In the open-loop state (Fig. 4), the densities of alpha particles, energy, hydrogen, and boron-11 particles decrease. The behaviors of total particles density, temperature and β for these states (open loop) are shown in Figures 6(*d, e, f*). A control system that incorporates one or more feedback paths is known as a Closed

Loop System. Closed Loop Control Systems are commonly used in managing processes as well as in electronic control applications. Feedback systems have part of their output signal fed back to the input for comparison with the desired set point condition. The kind of feedback signal may lead to either constructive feedback or detrimental feedback. Within a closed-loop system, a controller is employed to assess the system's output against the target condition and transform any discrepancies into control actions aimed at minimizing the error and restoring the system's output to the intended response. Subsequently, closed-loop control systems utilize feedback to assess the real input to the system and may incorporate multiple feedback loops.

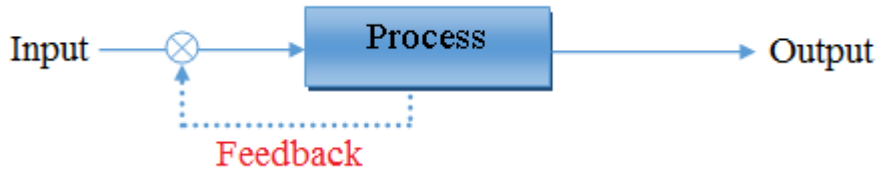

Figure 4. Close loop state

In a simulation of closed loop, the regulator must adjust fuel and thermal levels to achieve the ideal equilibrium of the system. Figure 5 (solid-blue) illustrates the progression of the states regarding densities and energy throughout the simulation, while Figures 6(*a, b, c*) depict the temporal changes in overall particle density, temperature, and β for the closed loop condition. Following a thermal fluctuation, the progression of densities and energy successfully converges to their target equilibrium levels.

Figure 7 illustrates how the actuator and fuel ratios change over time in a closed-loop state. These Figures demonstrate the variations in supplementary power, fuel injection rates, and fuel fractions over time to manage the system's energy. As shown in Figure 7, in this system supplementary power is nonzero at first and so system is controlled based on modulation of fueling rate and change of supplementary power (sub-ignition point).

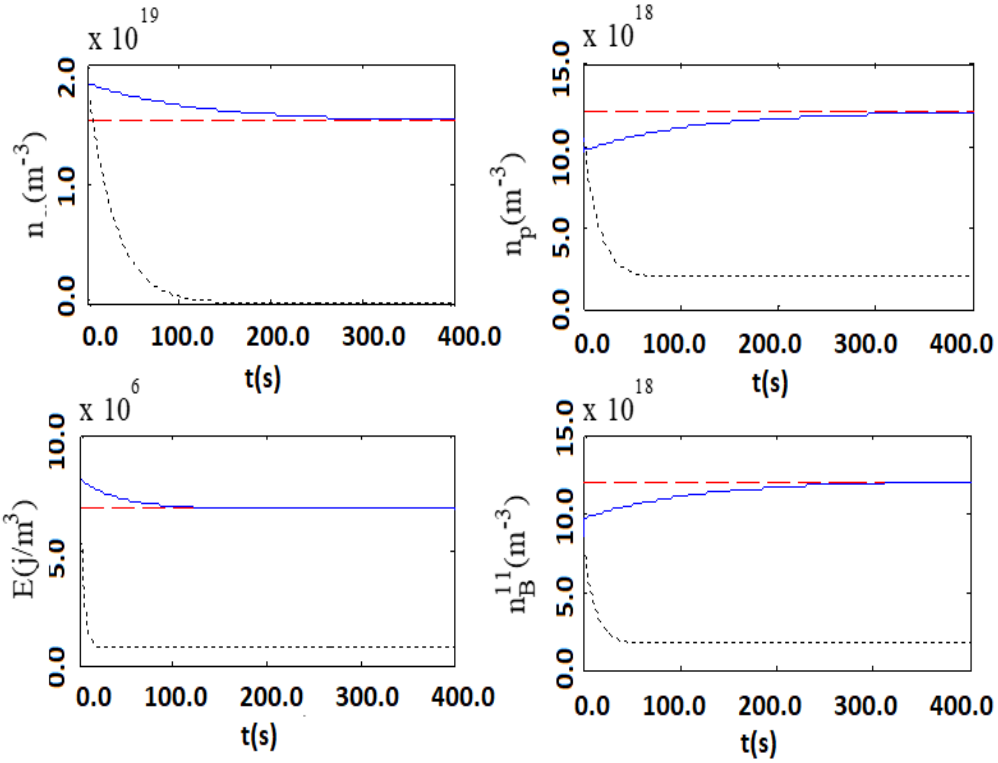

Figure 5. Time evolution of $p^{11}B$ fuel in open loop states (black-doted), close loop states (blue-solid) and equilibrium value (red-dashed)

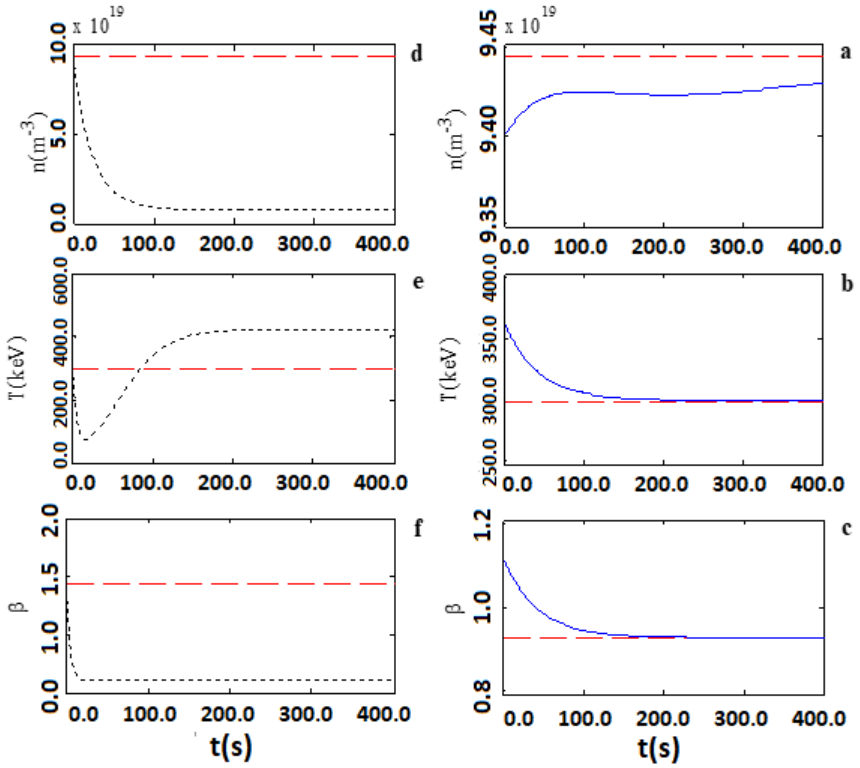

Figure 6. Time Evolution of T, n, β for $p^{11}B$ fuel, open loop (black-doted — *d*, *e*, *f*), close loop (blue-solid — *a*, *b*, *c*) and equilibrium values (red-dashed)

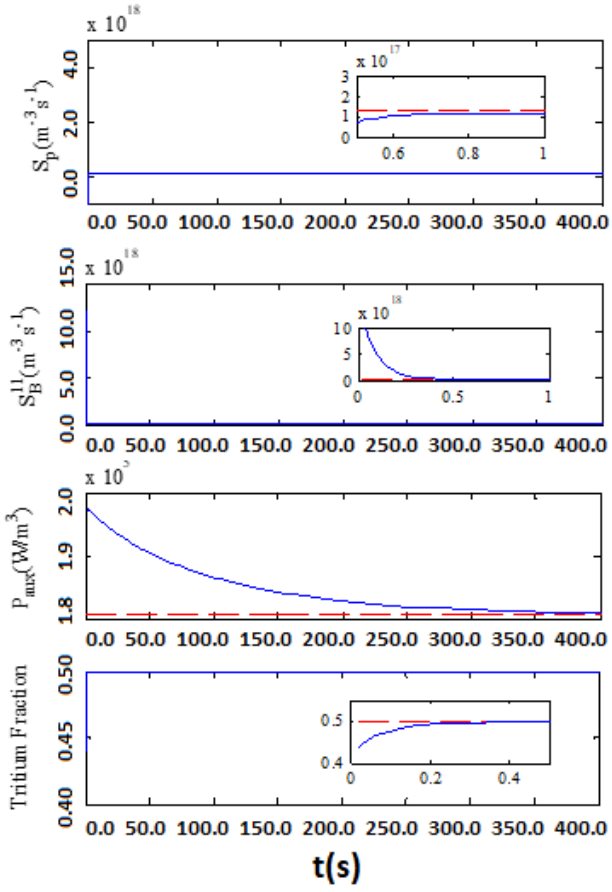

Figure 7. Actuation (blue-solid), equilibrium value (red-dashed) and Boron 11 Fraction for $p^{11}B$ fuel

Figure 8 shows the time evolutions of the fusion, radiation, ohmic and net plasma heating power which compared with equilibrium values. Fusion and ohmic heating power increases and radiation heating power decreases over time that as a result the net plasma heating power is close to the equilibrium value after time .04 s. The quality factor in fusion reactors is defined as:

$$Q = \frac{P_{fusion}}{P_{auxiliary}} \tag{36}$$

This factor is shown in Figure 9 and as be seen after time 300 s is close to .13.

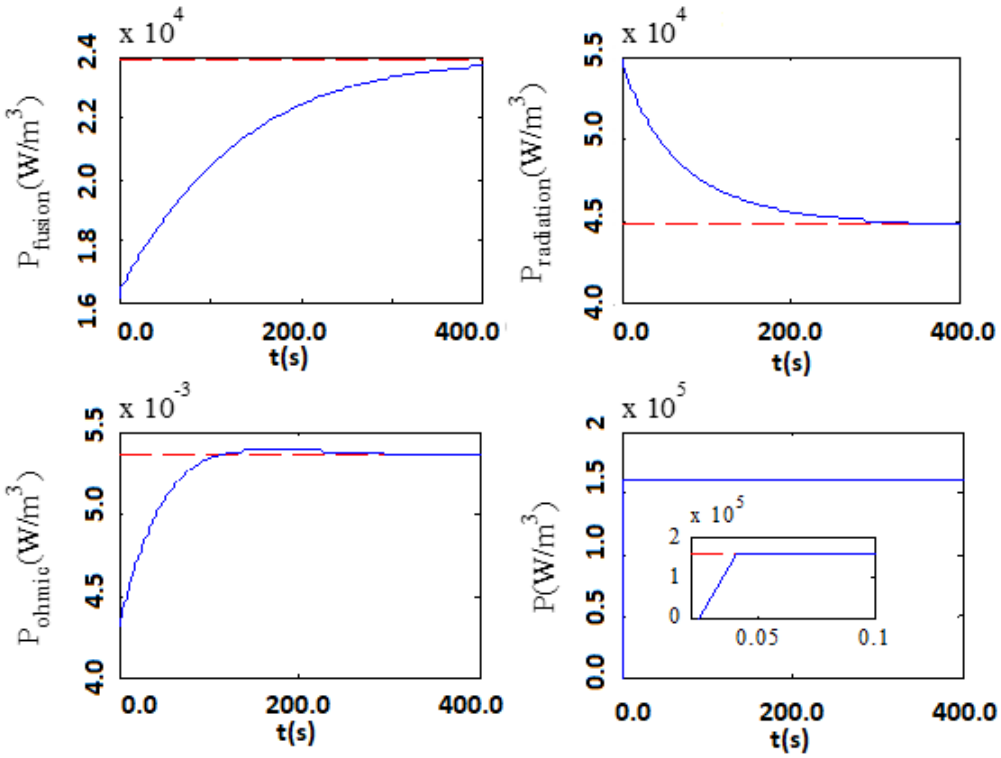

Figure 8. Fusion, radiation, ohmic, and overall Plasma heating power (shown in blue and solid) as opposed to their steady-state values (represented in red and dashed).

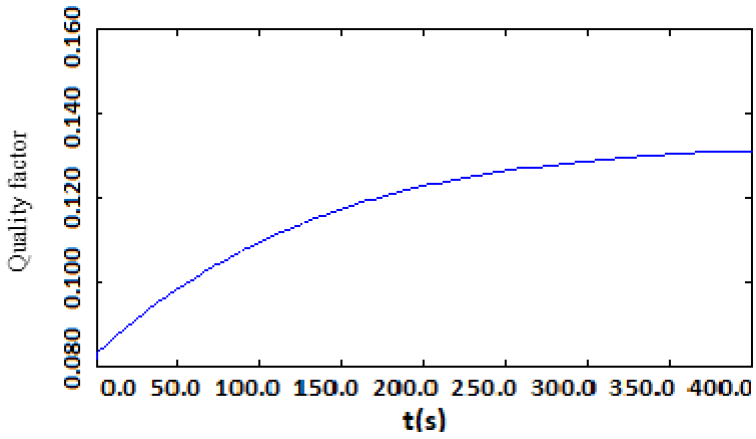

Figure 9. Time evolution of quality factor

Conclusions

In order to burning control, the supplementary power is put to zero initially and by changing the fueling rate and boron 11 fraction, system approaches to control values. Since the supplementary power is zero, system operates in ignition point and when the fueling rate approaches to its equilibrium value and the bo-

ron 11 – hydrogen ratio 50:50 the supplementary power should be added to control the system so this system operates in sub-ignition point and the system (energy and particles density) is controlled. In the case of $p^{11}B$ fuel the system is controlled by adding the supplementary power and since the supplementary power is non-zero the system operates in sub-ignition point and hydrogen – boron 11 ratio in primary times is equal to 50:50 (Fig. 6) and as a result system (energy and particles density) approaches to its equilibrium values.

Compared to a deuterium-tritium (DT) reactor, the lower neutron flux in a $p^{11}B$ reactor provides significant advantages in engineering, safety, and environmental impact, including:

1. There is no risk of structural melting during a loss-of-coolant incident.

2. The first wall does not need to be replaced frequently, which results in increased reactor uptime and greatly diminished radiation exposure for workers.

3. There is a significant decrease in tritium emissions and concerns regarding radioactive waste.

4. Tritium breeding is unnecessary, eliminating the need for a large lithium blanket and avoiding issues related to liquid metals.

References

1 Anand, H., Coda, S., Felici, F., Galperti, C., & Moret, J.-M. (2017). A novel plasma position and shape controller for advanced configuration development on the TCV tokamak. *Nucl. Fusion, 57*, 126026. DOI: 10.1088/1741-4326/aa7f4d

2 Mele, A. et al. (2019). MIMO shape control at the EAST tokamak: simulations and experiments. *Fusion Eng. Des., 146*, 1282–1285. DOI:10.1016/j.fusengdes.2019.02.058

3 Anand, H. et al. (2020). Plasma flux expansion control on the DIII-D tokamak. *Plasma Phys. Control Fusion, 63*, 015006. DOI.10.1088/1361-6587/abc457

4 De Tommasi, G. (2019). Plasma magnetic control in tokamak devices, *J. Fusion Energy, 38*, 406–436. DOI: 10.1007/s10894-018-0162-5

5 Blum, J., Heumann, H., Nardon, E., & Song, X. (2019). Automating the design of tokamak experiment scenarios. *J. Comput. Phys., 394*, 594–614. DOI: 10.1016/j.jcp.2019.05.046

6 Moret, J.-M. et al. (2015). Tokamak equilibrium reconstruction code LIUQE and its real time implementation. *Fusion Eng. Des., 91*, 1–15. DOI:10.1016/j.fusengdes.2014.09.019

7 Xie, Z., Berseth, G., Clary, P., Hurst, J. & van de Panne, M. (2018). Feedback control for Cassie with deep reinforcement learning. In *2018 IEEE/RSJ International Conference on Intelligent Robots and Systems (IROS) IEEE*, 1241–1246. DOI: 10.1109/IROS.2018.8593722

8 Jardin, S. (2010). *Computational Methods in Plasma Physics*, CRC Press. DOI: 10.1201/EBK1439810958

9 Bellemare, M. G. et al. (2020). Autonomous navigation of stratospheric balloons using reinforcement learning. *Nature, 588*, 77–82. DOI: 10.1038/s41586-020-2939-8

10 Humphreys, D. et al. (2020). Advancing fusion with machine learning research needs workshop report. *J. Fusion Energy, 39*, 123–155. DOI: 10.1007/s10894-020-00258-1

11 Joung, S. et al. (2019). Deep neural network Grad-Shafranov solver constrained with measured magnetic signals. *Nucl. Fusion, 60*, 16034. DOI: 10.1088/1741-4326/ab555f

12 van de Plassche, K. L. et al. (2020). Fast modeling of turbulent transport in fusion plasmas using neural networks. *Phys. Plasmas, 27*, 022310 .DOI: 10.1063/1.5134126

13 Abbate, J., Conlin, R., & Kolemen, E. (2020). Data-driven profile prediction for DIII-D. *Nucl. Fusion, 61*, 046027.DOI:10.1088/1741-4326/abe08d

14 Kates-Harbeck, J., Svyatkovskiy, A., & Tang, W. (2019). Predicting disruptive instabilities in controlled fusion plasmas through deep learning. *Nature, 568*, 526–531. DOI:10.1038/s41586-019-1116-4

15 Walker, M. L., & Humphreys, D.A. (2006). Valid coordinate systems for linearized plasma shape response models in tokamaks. *Fusion Sci. Technol., 50*, 473–489. DOI:10.13182/FST06-A1271

16 Austin, M. E. et al. (2019). Achievement of reactor-relevant performance in negative triangularity shape in the DIII-D tokamak. *Phys. Rev. Lett., 122*, 115001.DOI:10.1103/PhysRevLett.122.115001

17 Kolemen, E. et al. (2018). Initial development of the DIII-D snowflake divertor control. *Nucl. Fusion, 58*, 066007. DOI: 10.1088/1741-4326/aab0d3

18 Anand, H. et al. (2019). Real time magnetic control of the snowflake plasma configuration in the TCV tokamak. *Nucl. Fusion, 59*, 126032. DOI: 10.1088/1741-4326/ab4440

19 Wabersich, K. P., Hewing, L., Carron, A., & Zeilinger, M.N. (2021). Probabilistic model predictive safety certification for learning-based control. *IEEE Tran. Automat. Control, 67*, 176–188. DOI: 10.1109/TAC.2021.3049335

20 Abdolmaleki, A. et al. (2021). On multi-objective policy optimization as a tool for reinforcement learning. Preprint at https://arxiv.org/abs/2106.08199

С.Н. Хоссейнимотлаг, М.А. Зарей, А. Шакери

Альфа-протон-альфа көшкіні реакциясы механизмі арқылы нейтронсыз $p^{11}B$ отыны бар токамак термоядролық реакторында плазманы жағуды бақылау әдісі

Мақала нейтрондық отын проблемаларына арналған. Альфа-протон-альфа көшкіні реакциясы арқылы нейтронсыз $p^{11}B$ отыны бар токамак термоядролық реакторында плазманың жануын бақылаудың сипаттамалық ерекшеліктері талданған. Зерттеу негізінде авторлар бөлшектер мен энергия тепе-теңдігінің теңдеулері қолданылатын плазмалық тұтану өлшемдері жоқ модельді ұсынады. Осы модель шеңберінде $p^{11}B$ отыны қарастырылған. Шын мәнінде, бұл жұмыс жанып жатқан плазманы басқарудың жаңа әдісін ұсынады, осылайша жүйенің өзгеруін, жанармай құю жылдамдығын және қосымша қуатты басқаруға болады. Модельдеу теңдеулерін қолдана отырып, $p^{11}B$ отынының сапа коэффициенті есептелді. Нейтрондық отынның екі негізгі кемшілігі бар: (i) олар қорғауды қажет ететін және реактордың құрылымына зиян келтіретін және белсендіретін нейтрондарды шығарады, (ii) тритий өндірісі қосымша күрделілікті, шығындарды және литий жабыны үшін радиалды кеңістіктің қажеттілігін қамтиды. Нейтронсыз $p^{11}B$ реакциясы көбінесе осы мәселелерді шешудің әлеуетті құралы ретінде қарастырылатыны көрсетілген.

Кілт сөздер: плазма, термоядролық синтез, динамика, нейтронсыз, энергия, бақылау, көшкін, альфа, протон, отын

С.Н. Хоссейнимотлаг, М.А. Зарей, А. Шакери

Способ управления горением плазмы в термоядерном реакторе токамак на безнейтронном топливе $p^{11}B$ по механизму альфа-протон-альфа лавинной реакции

Статья посвящена проблемам нейтронного топлива. Проанализированы характерные особенности управления горением плазмы в термоядерном реакторе токамак с использованием безнейтронного топлива $p^{11}B$ посредством лавинной реакции альфа-протон-альфа. На основе проведенного исследования авторы предлагают безразмерную модель зажигания плазмы, в которой используются уравнения равновесия частиц и энергии. В рамках этой модели рассматривается топливо $p^{11}B$. В работе представлен новый метод управления горящей плазмой, позволяющий контролировать изменения в системе, скорость заправки топливом и дополнительную мощность. Применяя уравнения моделирования, былл рассчитан коэффициент качества топлива $p^{11}B$. У нейтронного топлива есть два основных недостатка: (i) оно генерирует нейтроны, которые требуют защиты и могут повредить конструкцию реактора и активировать ее, (ii) производство трития сопряжено с дополнительной сложностью, расходами и необходимостью в радиальном пространстве для литиевого покрытия. Показано, что безнейтронная реакция $p^{11}B$ часто рассматривается как потенциальное решение этих проблем.

Ключевые слова: плазма, термоядерный синтез, динамика, без нейтронов, энергия, управление, лавина, альфа, протон, топливо

Information about the authors

Seyede Nasrin Hosseinimotlagh — Doctor of Physics, Leading Researcher, Department of Physics, Shi.C., Islamic Azad University, Shiraz, Iran; e-mail: nasrinhosseini_motlagh@iau.ir; https://orcid.org/0000-0001-5381-2449;

Mohammad Ali Zarei — Doctor of Physics, Senior Researcher, Department of Physics, Payame Noor University, Tehran, Iran; e-mail: M.Zarei2345@gmail.com;

Abuzar Shakeri (*contact person*) — Doctor of Technical Sciences, Senior Researcher, Department of Physics, Shi. C., Islamic Azad University, Shiraz, Iran e-mail: Abuzar.Shakeri6845@gmail.com; https://orcid.org/0009-0007-8075-6711